Chemical Science

ROYAL SOCIETY OF CHEMISTRY

EDGE ARTICLE

View Article Online
View Journal | View Issue

Cite this: *Chem. Sci.*, 2022, **13**, 9016

All publication charges for this article have been paid for by the Royal Society of Chemistry

Adaptive coordination assemblies based on a flexible tetraazacyclododecane ligand for promoting carbon dioxide fixation†

Shaochuan Li,[ab] Caiping Liu,[a] Qihui Chen, *[a] Feilong Jiang,[a] Daqiang Yuan, [a] Qing-Fu Sun *[a] and Maochun Hong *[a]

Received 2nd June 2022
Accepted 4th July 2022

DOI: 10.1039/d2sc03093d

rsc.li/chemical-science

Coordination hosts based on flexible ligands have received increasing attention due to their inherent adaptive cavities that often show induced-fit guest binding and catalysis like enzymes. Herein, we report the controlled self-assembly of a series of homo/heterometallic coordination hosts $(Me_4enPd)_{2n}(\mathbf{ML})_n$ [n = 2/3; M = Zn(II)/Co(II)/Ni(II)/Cu(II)/Pd(II)/Ag(I); Me_4en: *N*,*N*,*N*′,*N*′-tetramethylethylenediamine] with different shapes (tube/cage) from a flexible tetraazacyclododecane-based pyridinyl ligand (**L**) and *cis*-blocking Me_4enPd(II) units. While the Ag(I)-metalated ligand (**AgL**) gave rise to the formation of a $(Me_4enPd)_4(\mathbf{ML})_2$-type cage, all other M(II) ions led to isostructural $(Me_4enPd)_6(\mathbf{ML})_3$-type tubular complexes. Structural transformations between cages and tubes could be realized through transmetalation of the ligand. The buffering effect on the **ML** panels endows the coordination tubes with remarkable acid–base resistance, which makes the $(Me_4enPd)_6(\mathbf{ZnL})_3$ host an effective catalyst for the CO_2 to CO_3^{2-} conversion. Control experiments suggested that the integration of multiple active Zn(II) sites on the tubular host and the perfect geometry match between CO_3^{2-} and the cavity synergistically promoted such a conversion. Our results provide an important strategy for the design of adaptive coordination hosts to achieve efficient carbon fixation.

Introduction

Carbon dioxide (CO_2) in the atmosphere has been rising due to humans' reliance on fossil fuels, causing a range of climate problems such as rising temperature and changing sea-levels. To eliminate such problems, it is necessary to develop efficient and economic carbon fixation technologies.[1,2] In order to transform CO_2 into valuable compounds, various carbon fixation technologies such as metal-participated chemical conversions,[3] electrocatalysis,[4] and photocatalysis[5,6] have been developed. Ideally, the carbon fixation process itself should avoid CO_2 emissions to achieve carbon neutralization. However, it remains a big challenge to develop such carbon fixation processes.

In nature, carbonic anhydrase can convert CO_2 into HCO_3^- under mild conditions. Structural analysis shows that carbonic anhydrase contains a flexible cavity that can hold CO_2 and a coordination unsaturated Zn(II) ion acting as the active site.[7,8] Inspired by this, many unusual metal complexes which can be used to fix CO_2 through binding with carbonate have been reported.[9–13] Coordination-directed self-assembly has been proven to be an effective approach toward the predictable construction of multicomponent artificial hosts,[14–77] where enhanced guest reactivity,[73,74,78–87] stabilization of metastable species,[88–90] and unusual reaction pathways[78,91–94] have been realized. While atmospheric CO_2 sequestration by selective binding of carbonate with coordination hosts has already been reported,[95–102] adaptive coordination hosts that contain multiple active metal sites and can reversibly encapsulate and release the carbonate are still rare.

1,4,7,10-Tetraazacyclododecane and its derivatives are well-studied macrocyclic ligands to form stable complexes with various metal ions.[103–106] However, its utilization in coordination-directed self-assembly has been hampered due to its structural flexibility.[21,23] Herein, we report the synthesis of a series of coordination tubes or cages from a 1,4,7,10-tetraazacyclododecane-*N*,*N*′,*N*″,*N*‴-tetra-*p*-methylpyridine ligand (**L**) and *cis*-blocking Me_4enPd units (Scheme 1). The structure of the final assemblies is found to be sensitive to different metallations on **L**. Moreover, integration of multiple active Zn(II) sites on the $(Me_4enPd)_6(\mathbf{ZnL})_3(NO_3)_{18}$ (**1-Zn**) tubular host and perfect CO_3^{2-} encapsulation in the cavity promoted its potential utilization in CO_2 fixation.

[a]*State Key Laboratory of Structure Chemistry, Fujian Institute of Research on the Structure of Matter, Chinese Academy of Sciences. Fuzhou, Fujian, 350002, China. E-mail: chenqh@fjirsm.ac.cn; qfsun@fjirsm.ac.cn; hmc@fjirsm.ac.cn*

[b]*University of the Chinese Academy of Sciences, Beijing, 100049, China*

† Electronic supplementary information (ESI) available. CCDC 213469, 213472–213476, 213485–213486, 2131470–2131471. For ESI and crystallographic data in CIF or other electronic format see https://doi.org/10.1039/d2sc03093d

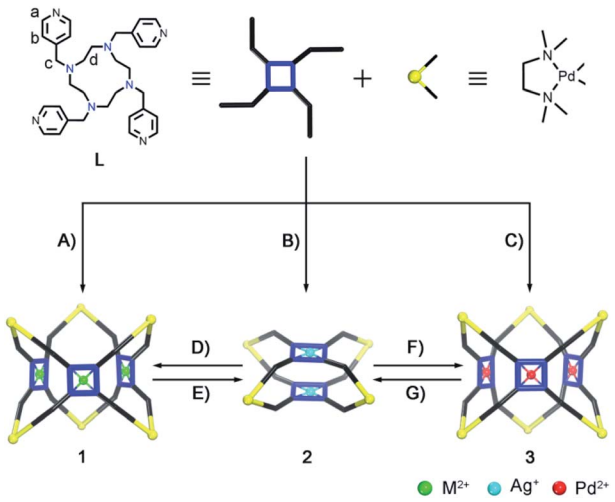

Scheme 1 Controlled self-assembly and transformations between coordination cages and tubes. (A) Coordination tubes $[(PdMe_4en)_6(ML)_3]^{18+}$ (**1-M**) (M = Zn, Co, Ni, Cu) by metallation of **L** with M(II). (B) Coordination cages $[(PdMe_4en)_4(AgL)_2]^{12+}$ (**2**) by metallation of **L** with Ag(I). (C) Coordination tubes $[(PdMe_4en)_6(PdL)_3]^{18+}$ (**3**) by metallation of **L** with Pd(II). (D) Zn(II) induced transformation from **2** to **1-Zn**. (E) Ag(I) driven transformation from tube **1-Zn** to **2**. (F) Pd(II) induced transformation from cage **2** to **3**. (G) Ag(I) driven transformation from **3** to **2**.

Results and discussion

Controlled self-assembly and structural transformations between coordination tubes 1 and 3, and cages 2

The tetraazacyclododecane moiety located at the center of ligand **L** is prone to being metalated due to the macrocyclic effect. Indeed, treatment of **L** with $Zn(NO_3)_2$ led to the quantitative formation of the **ZnL** metalloligand, as confirmed by ^{1}HNMR (Fig. 1A and B, S1–S8†) and single crystal X-ray diffraction (SCXRD) studies. In the ^{1}HNMR spectrum of **ZnL**, the signal of H_d is not only down-field shifted but also splits into two peaks, suggesting that metallation of **L** by Zn(II) rigidified its conformation in solution. In the crystal structure, four pyridine groups on **ZnL** are in the same plane rather than the randomly distributed form seen on the free **L** (Fig. 2A and B, S9 and S10†). Reacting $Me_4enPd(NO_3)_2$ with **ZnL** in D_2O at 70 °C for 3 h led to formation of one clean complex (**1-Zn**). ^{1}HNMR analyses show that both the signals of H_a and H_b on **1-Zn** shift to the down-field than that on **ZnL**, due to the coordination of pyridine groups to Pd(II) (Fig. 1C, S11–S13†). Diffusion ordered NMR spectroscopy (DOSY) further indicates the purity and the size (about 2.1 nm) of **1-Zn** (Fig. S14†). The X-ray crystal structure of **1-Zn** was also obtained, which clearly confirmed its tubular structure $[(Me_4enPd)_6(ZnL)_3]^{18+}$ (Fig. 2C, S15†). Six Pd(II) capping units are located on the six vertices of the triangular prism, while three **ZnL** ligands define the three faces of the triangular prism, with one NO_3^- encapsulated in the tubular cavity. The chelated Zn(II) ion displays a tetragonal pyramid geometry through coordinating with four N atoms from **L** and one O atom from water. Such coordination mode makes the new-formed metalloligand **ZnL** adopt the planar conformation, leading to the formation of a tubular structure. The triangular apertures on the tube are about 13.7 Å × 13.7 Å × 13.7 Å. No

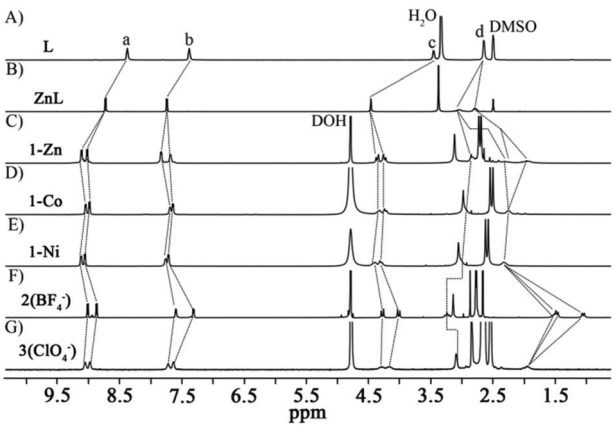

Fig. 1 ^{1}HNMR spectra of (A) free ligand **L**, (B) **ZnL**, (C) **1-Zn**, (D) **1-Co**, (E) **1-Ni**, (F) **2**(BF_4^-), and (G) **3**(ClO_4^-).

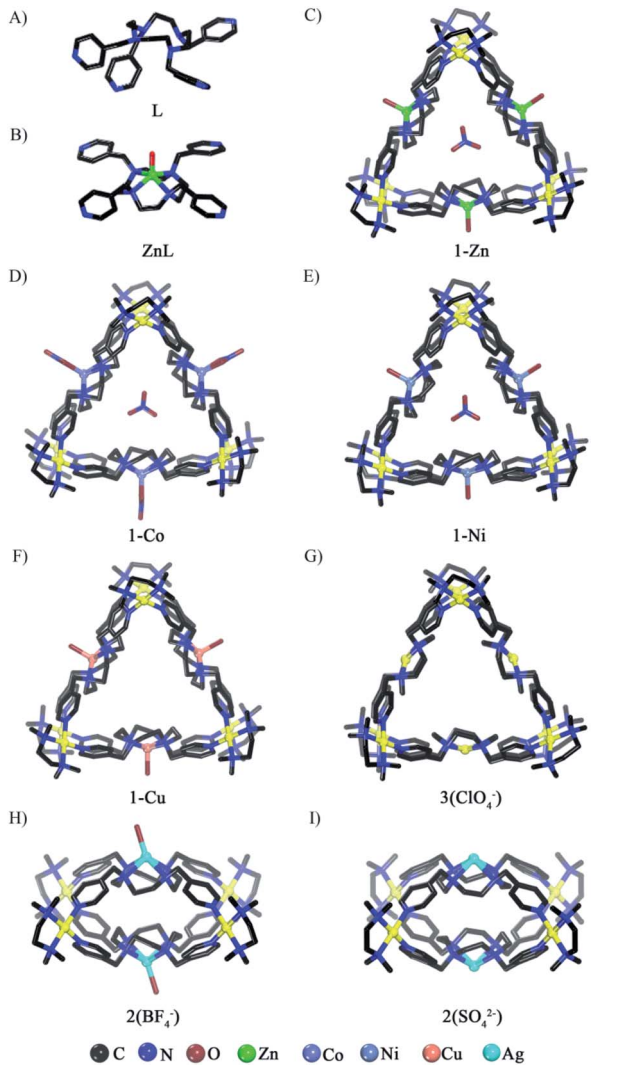

Fig. 2 The crystal structures of (A) free ligand **L**, (B) **ZnL**, (C) **1-Zn**, (D) **1-Co**, (E) **1-Ni**, (F) **1-Cu**, (G) **3**(ClO_4^-), (H) **2**(BF_4^-), and (I) **2**(SO_4^{2-}).

anion effect was observed on the self-assembly of tube **1-Zn**, as isostructural tubular complexes were obtained using other Me_4enPd (BF_4^-, SO_4^{2-}, ClO_4^-, SbF_6^- salts) (Fig. S16–S20†). One-pot self-assembly starting from **L**, $Zn(NO_3)_2$ and Me_4enPd salt also leads to the coordination tube **1-Zn** (Fig. S21†).

When other transition metal ions M(II) (M = Co, Ni, Cu) that can adopt similar coordination geometries to Zn(II) ions were used, heterometallic coordination tubes $[(Me_4enPd)_6(ML)_3]^{18+}$ [M = Co^{2+} (**1-Co**), Ni^{2+} (**1-Ni**), Cu^{2+} (**1-Cu**)] were obtained (Fig. 1D and E, S22–S27†). SCXRD analyses confirm that complexes **1-Ni** and **1-Cu** are isostructural to tube **1-Zn**, except that no NO_3^- can be found in the cavity of **1-Cu** (Fig. 2E and F, S29 and S30†). Although the chelated Co(II) ion in **1-Co** displays a distorted octahedral configuration, it has the same coordination form with the ligand **L** as the Zn(II), so the Co(II) ion also induces the formation of a tubular structure (Fig. 2D, S28†). In short, Zn(II)/Co(II)/Ni(II)/Cu(II) ions can be used as templates to induce the self-assembly of heterometallic tubular tubes (**1-M**) because they can drive the metalloligand **ML**s to adopt a planar conformation (Scheme 1A).

To our surprise, cage complexes **2** were obtained by the *in situ* self-assembly of **L**, $PdMe_4en(Cl)_2$ and AgX (X = BF_4^-, SO_4^{2-}), as confirmed by ^{1}H and DOSY NMR spectra (Fig. 1F, S31–S34 and S36–S39†). The ^{1}HNMR spectrum of **2**(BF_4^-) is distinct from that of **1** (Fig. 1C and F). DOSY shows that the size of **2** is about 1.28 nm (Fig. S34 and S39†), much smaller than that of **1**. SCXRD confirmed that **2** complexes with different counter ions (either BF_4^- or SO_4^{2-}) are isostructural coordination cages with the same $[(PdMe_4en)_4(AgL)_2]^{12+}$ skeleton (Fig. 2H and I). The crystal structures of **2** show that all the ligands **L** became the metalated **AgL**. Both structures are composed of two **AgL** ligands and four Pd(II) nodes with almost no cavity observed (Fig. S35 and S40†). The coordination environments of the Ag(I) centers on the **AgL** ligands of **2** (BF_4^- salt) and **2** (SO_4^{2-} salt) are similar except that one additional axial coordinating H_2O was observed on the former (Fig. 2H and I). The longer Ag–N bond length (2.5 Å on average) compared to that of Zn–N (2.1 Å on average) leads to a slight conical conformation of **AgL** other than the flat conformation observed for **ZnL**. This conformational change on **AgL** leads to the formation of the cage structure. Isostructural cages **2** (NO_3^-, ClO_4^-) also could be obtained when $AgNO_3$ and $AgClO_4$ were used (Fig. S41†), further confirming that Ag(I) ions can template the self-assembly of coordination cages (**2**) (Scheme 1B).

It then turns out that the metallation of **L** was a prerequisite for the successful self-assembly. Trail on direct self-assembly of **L** with $Me_4enPd(NO_3)_2$ gave a mixture of products (Fig. S42 and S43†). Interestingly, reacting ligand **L** with $Me_4enPd(ClO_4)_2$ led to a new $(Me_4enPd)_6(PdL)_3$-type tube complex (**3**), with the *in situ* metallation of **L** with Pd(II). The ^{1}HNMR spectrum of **3** is clearly different from those of both **1** and **2** (Fig. 1G and S44–S46†). DOSY shows that the size of **3**(ClO_4^-) is about 2.2 nm (Fig. S47†), very close to that of tube **1-Zn**. SCXRD finally confirms that **3**(ClO_4^-) is a Pd-chelated triangular coordination tube $[(Me_4enPd)_6(PdL)_3](ClO_4)_{18}$ (Fig. 2G, S48†). The crystal structure of **3**(ClO_4^-) contains two independent tubular molecules. Both of them have a triangular prism structure similar to that of **1-Zn**, where six Pd nodes are located on six vertices of the triangular prism and three **PdL** metalloligands span three faces of the prism. The Pd(II) ions chelated in the **PdL** ligands adopt the square-planar coordination geometry. Like **ZnL**, **PdL** also adopts a planar conformation, so a similar tube complex is formed. A clean tubular complex **3** (SbF_6^- salt) could also be obtained when $Me_4enPd(SbF_6)_2$ was used (Fig. S49–S52†). However, both $Me_4enPd(BF_4)_2$ and $Me_4enPdSO_4$ lead to a mixture of products, demonstrating an obvious anionic effect (Fig. S53†).

With the structure of hetero/homometallic coordination tubes **1** and **3**, and cages **2** determined, we then wondered whether controllable structural transformation between cages and tubes can be achieved through transmetalation on the **ML**. Indeed, the addition of Zn(II) ions to the Ag-chelated cage **2** triggered its complete transformation into Zn-chelated tube **1-Zn** (Fig. S54–S56†). Due to the much stronger coordination ability of Zn(II) than Ag(I) with **L**, it is difficult for Ag(I) ions to drive the back transformation. Even with a large excess of Ag(I) ions, only a partial transformation from tube **1-Zn** to cage **2** was observed (Fig. S57–S59†). Similarly, cage **2** can be completely transformed into tube **3** by the addition of Pd(II) salts, where use of $Pd(SbF_6)_2$ can greatly promote this transformation (Fig. S60–S62†), while back transformation from tube **3** to cage **2** is successful by the addition of $AgBF_4$ or $AgNO_3$, but not for $AgSbF_6$ (Fig. S63–S65†). We infer that SbF_6^- may have a stronger interaction with tube **3** than cage **2**, so it can promote the conversion of cage **2** to tube **3** but hamper the back transformation. In brief, controllable transformations between cages and tubes can be realized *via* transmetalation on the ligands with a certain degree of anion effects (Scheme 1D–G).

Fine-tuned shapes and cavities on the tubular complexes

It's worth noting that the utilization of the flexible tetraazacyclododecane-based ligand not only facilitates the incorporation of various metal ions on the coordination tubes, but also provides a good opportunity to fine-tune the volumes of their central cavities. Based on the crystal data, deformations of geometry on **L** depending on its metallation with different metal ions are clearly observed, leading to gradual volume changes from 316 (**1-Ni**) to 409 [**3**(ClO_4^-)] Å^3 (Fig. 3B). For the isostructural heterometallic tubes **1-Zn**/**Ni**/**Cu**, their central metals share the same coordination environment, and the volumes of the tubes are found to be proportional to the M–N bond lengths on **ML**s (**N-Ni** < **N-Cu** < **N-Zn**). We infer that shorter coordination bonds make the **ML**s panels more convex, while such conformational changes do not cause significant changes to the triangular opening (Fig. 3A). **1-Co** and **3**(ClO_4^-) with quite different coordination environments on **ML**s bear much larger volumes than the above three tubes, with the largest volume of 409 Å^3 measured for tube **3**(ClO_4^-), which is *ca.* 1.3 times that for **1-Ni**. We infer that the volume increases in these two tubes are due to their less curved **ML** panels.

Acid–base resistance of coordination tubes

Stability of the coordination assemblies is an important prerequisite for their applications.[21,23] Impressively, ^{1}H-NMR for

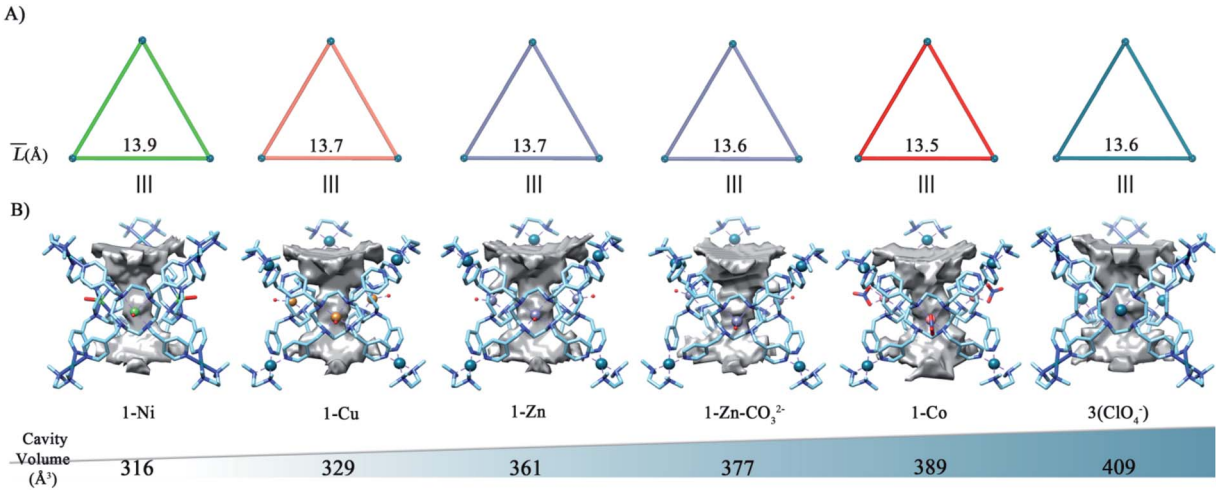

Fig. 3 (A) The average lengths of triangular apertures on different tubular structures. (B) The volumes of cavities on tubes **1-Ni** (316 Å^3), **1-Cu** (329 Å^3), **1-Zn** (361 Å^3), **1-Zn-CO$_3$$^{2-}$** (377 Å^3), **1-Co** (389 Å^3), and **3**(ClO_4^-) (409 Å^3).

tube **1-Zn** in aqueous solutions confirmed that it maintained its structural integrity under both strongly acidic (pH = 1) and basic conditions (pH = 12) but would decompose in stronger acidic (pH = 0) or basic (pH = 13) solutions (Fig. S66†). Tubes **1-Co** and **1-Ni** also remain stable at pH 12, but their acid resistance is poorer than that of **1-Zn** (Fig. S67 and S68†). For comparison, a simple coordination complex (Me_4enPd)$Py_2(NO_3)_2$ (Py = pyridine) was synthesized. ^{1}H-NMR tests indicate that it can only remain intact in a smaller pH range (pH 3–11; Fig. S69†), suggesting that multi-component cooperativity on the tube enhances its structural stability. The buffering effect of **ML**, *i.e.*, accepting H^+ on the N atoms of tetraazacyclododecane and OH^- on the metal centers *via* axial coordination, should also contribute to the observed acid–base resistance of the tube complexes. While many acid or base resistant coordination hosts have been reported, few of them are stable toward both acidic and basic conditions. Coordination hosts built from inert coordination bonds, such as Pt–N, and Zr–O bonds, tend to show enhanced stability.[107,108] Compared with the strategy of using stronger coordination bonds, here we improve the acid–base stability of the host by creating a local buffer environment, which provides a useful strategy for the construction of stable coordination hosts.

CO_2 fixation promoted by coordination tubes

Considering that the coordination tube **1-Zn** contains three Zn active sites and is tolerable toward basic solutions, we then studied its applications in carbonic anhydrase mimicking. The CO_2 dissolution experiment indicates that CO_2 has better solubility in DMSO/H_2O (1 : 2 v/v) mixed solvent than pure water (Fig. S70†). So, a DMSO-d_6/D_2O mixed solvent containing **1-Zn** (5 mM) and NaOH (0.01 M) was used for the CO_2 capture reaction. When CO_2 gas was continuously injected into this solution at room temperature for 3 h, a signal at 160 ppm assignable to CO_3^{2-} was clearly observed in ^{13}CNMR (Fig. 4B(c) and (d)), whereas no CO_3^{2-} was observed without adding **1-Zn**, or with **1-Co**, **1-Ni** as the catalysts (Fig. 4B(a) and (b), S71†). A control experiment with a mononuclear **ZnL^1(NO$_3$)$_2$** (**L^1** = 1,4,7,10-tetraazacyclododecane) complex as the catalyst, which contains a similar Zn(II) active site, also showed no CO_2 conversion (Fig. S72–S74†). Taking together all these experiments, it is clear that both the existence of the Zn metal sites

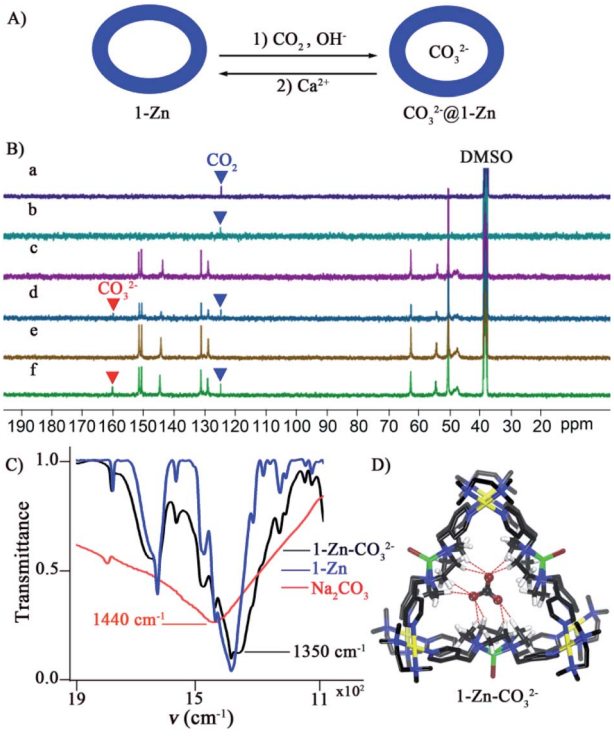

Fig. 4 (A) The **1-Zn** tube assisted CO_2 to CO_3^{2-} conversion. (B) The ^{13}C NMR spectra of CO_2 (a), the blank experiment (b), **1-Zn** (c) and **1-Zn** promoted CO_2 to CO_3^{2-} transformation (d), after removing CO_3^{2-} with Ca^{2+} (e), and reuse of tube **1-Zn** (f). (C) The IR spectra of tube **1-Zn** before and after CO_2 fixation. (D) The crystal structure of **1-Zn-CO$_3$$^{2-}$**.

and the formation of the tubular cavity are indispensable to facilitate the CO_2 to CO_3^{2-} conversion.

Further studies indicate that adding more NaOH and prolonging the reaction time cannot enhance the yield of CO_3^{2-} in solution (Fig. S75†). The IR spectra of tube **1-Zn** after the reaction show a new absorption peak at 1350 cm^{-1}, which is obviously red-shifted compared with that in Na_2CO_3 (~1440 cm^{-1}) (Fig. 4C, S76†). The crystal of the **1-Zn-CO_3^{2-}** host–guest complex was obtained through slowly diffusing THF vapor into the reaction system. SCXRD confirmed that one CO_3^{2-} is tightly captured inside the tube cavity. Encapsulation of CO_3^{2-} also causes induced-fit cavity deformations, with the size of the triangular window changing to 13.1 Å × 13.6 Å × 14.0 Å and the volume increasing to 377 $Å^3$ compared to that of **1-Zn** (Fig. 3B, S77†). Multiple hydrogen bonds and the existence of strong electrostatic interactions lead to a strong host–guest interaction between CO_3^{2-} and the **1-Zn** host (Fig. 4D). We speculate that the formed **1-Zn-CO_3^{2-}** host–guest complex is inactive and hinders the turnover of further CO_2 conversion. Considering that Ca(II) ions can react with CO_3^{2-} to produce water-insoluble $CaCO_3$ ($K_{sp} = 2.80 \times 10^{-9}$), they have been used to grab the CO_3^{2-} encapsulated inside cavity. Further experiments showed that after removal of CO_3^{2-} encapsulated by the cavity, the tube **1-Zn** can be regenerated and reused (Fig. 4B(e) and (f)). Although many coordination hosts that can fix CO_2 by binding with carbonate have been reported,[95–102] the newly formed strong metal–oxygen interactions make these hosts unable to be reused. Thus, tube **1-Zn** represents a rare coordination host that can catalyze CO_2 conversion like carbonic anhydrase. In short, efficient and mild CO_2 conversion like the carbonic anhydrase can be realized by using an acid–base resistant coordination tube **1-Zn** (Fig. 4A). While the efficiency is weaker, our complex is much cheaper and can tolerate harsh conditions.

A possible cavity-assisted CO_2 conversion process was proposed as follows (Fig. S78†): (1) Zn(II) ions in tube **1-Zn** are coordination unsaturated, which can coordinate with OH^- to form Zn–OH units under basic conditions; (2) The Zn–OH group attacks the CO_2 in solution to form HCO_3^-, which is the rate-determining step of the conversion of CO_2. Compared to the OH^- coordinated to harder Co(II) and Ni(II), the enhanced nucleophilicity of Zn–OH makes it more efficient to attack CO_2; (3) HCO_3^- deprotonates into CO_3^{2-} due to the pK_a-shifting effect inside the cavity of the highly charged cationic host.[109] In fact, DFT calculations show that the $CO_3^{2-}\subset$**1-Zn** host–guest complexation energy was as high as −1349 kJ mol^{-1}; (4) the CO_3^{2-} sequestration by Ca(II) achieves the recycle of the catalyst and facilitates the reaction turnover.

Conclusions

A series of homo/heterometallic coordination assemblies have been synthesized from a tetraazacyclododecane-based ligand. Both self-assembly and structural transformations of coordination tubes/cages can be controlled in a cooperative manner using metal templates and auxiliary anions. The tubular complexes show adaptive cavities depending on the metallation of the ligand and the anions. The Zn-containing heteroleptic tubular complex not only shows impressive acid–base stability but also can catalyze the CO_2 to CO_3^{2-} conversion, standing for a rare example of an efficient and recyclable carbonic anhydrase-mimicking supramolecular system. Mechanistic studies confirm that the integration of multiple active metal sites and an open CO_3^{2-}-binding pocket is important for the CO_2 fixation. This work not only offers a new ligand candidate for the self-assembly of multi-variant coordination hosts, but also provides an important principle for the design of supramolecular catalysts toward CO_2 fixation.

Data availability

All experimental and computational data associated with this work are available in the ESI.†

Author contributions

S. Li and C. Liu performed the experiments. F. Jiang and D. Yuan helped with data analysis. Q. Chen, Q.-F. Sun, and M. Hong designed the project. All authors were involved in the preparation of the manuscript.

Conflicts of interest

There are no conflicts to declare.

Acknowledgements

This work was supported by the National Key Research and Development Program of China (2021YFA1500400, 2018YFA0704500, and 2017YFA0206800), the Key Research Program of Frontier Science CAS (QYZDY-SSW-SLH025), and the National Natural Science Foundation of China (21871265, 21731006, and 21825107).

Notes and references

1 C. Hepburn, E. Adlen, J. Beddington, E. A. Carter, S. Fuss, N. Mac Dowell, J. C. Minx, P. Smith and C. K. Williams, *Nature*, 2019, **575**, 87–97.
2 G. Mezei, *Chem*, 2019, **5**, 499–501.
3 L. Liang, C. Liu, F. Jiang, Q. Chen, L. Zhang, H. Xue, H.-L. Jiang, J. Qian, D. Yuan and M. Hong, *Nat. Commun.*, 2017, **8**, 1233.
4 L. Jiao, J. Zhu, Y. Zhang, W. Yang, S. Zhou, A. Li, C. Xie, X. Zheng, W. Zhou, S.-H. Yu and H.-L. Jiang, *J. Am. Chem. Soc.*, 2021, **143**, 19417–19424.
5 L. L. Ling, W. Yang, P. Yan, M. Wang and H. L. Jiang, *Angew. Chem., Int. Ed.*, 2022, **61**, e202116396.
6 T. Ouyang, H.-J. Wang, H.-H. Huang, J.-W. Wang, S. Guo, W.-J. Liu, D.-C. Zhong and T.-B. Lu, *Angew. Chem., Int. Ed.*, 2018, **57**, 16480–16485.
7 K. K. Kannan, B. Notstrand, K. Fridborg, S. Lövgren, A. Ohlsson and M. Petef, *Proc. Natl. Acad. Sci. USA*, 1975, **72**, 51–55.
8 P. Woolley, *Nature*, 1975, **258**, 677–682.

9 E. Garcia-Espana, P. Gavina, J. Latorre, C. Soriano and B. A. Verdejo, *J. Am. Chem. Soc.*, 2004, **126**, 5082–5083.
10 B. Verdejo, J. Aguilar, E. Garcia-Espana, P. Gavina, J. Latorre, C. Soriano, J. M. Llinares and A. Domenech, *Inorg. Chem.*, 2006, **45**, 3803–3815.
11 J.-M. Chen, W. Wei, X.-L. Feng and T.-B. Lu, *Chem.–Asian J.*, 2007, **2**, 710–719.
12 P. Mukherjee, M. G. B. Drew, M. Estrader and A. Ghosh, *Inorg. Chem.*, 2008, **47**, 7784–7791.
13 X. Liu, P. Du and R. Cao, *Nat. Commun.*, 2013, **4**, 2375.
14 M. Fujita, M. Tominaga, A. Hori and B. Therrien, *Acc. Chem. Res.*, 2005, **38**, 369–378.
15 M. D. Ward, C. A. Hunter and N. H. Williams, *Acc. Chem. Res.*, 2018, **51**, 2073–2082.
16 S. Pullen and G. H. Clever, *Acc. Chem. Res.*, 2018, **51**, 3052–3064.
17 M. Pan, K. Wu, J.-H. Zhang and C.-Y. Su, *Coord. Chem. Rev.*, 2019, **378**, 333–349.
18 J. Dong, Y. Liu and Y. Cui, *Acc. Chem. Res.*, 2021, **54**, 194–206.
19 L. Chen, Q. Chen, M. Wu, F. Jiang and M. Hong, *Acc. Chem. Res.*, 2015, **48**, 201–210.
20 D. L. Caulder and K. N. Raymond, *Acc. Chem. Res.*, 1999, **32**, 975–982.
21 T. R. Cook and P. J. Stang, *Chem. Rev.*, 2015, **115**, 7001–7045.
22 Y. Lu, H.-N. Zhang and G.-X. Jin, *Acc. Chem. Res.*, 2018, **51**, 2148–2158.
23 E. G. Percastegui, T. K. Ronson and J. R. Nitschke, *Chem. Rev.*, 2020, **120**, 13480–13544.
24 S. M. Jansze and K. Severin, *Acc. Chem. Res.*, 2018, **51**, 2139–2147.
25 M. Yoshizawa and L. Catti, *Acc. Chem. Res.*, 2019, **52**, 2392–2404.
26 H. Kumari, C. A. Deakyne and J. L. Atwood, *Acc. Chem. Res.*, 2014, **47**, 3080–3088.
27 L. J. Jongkind, X. Caumes, A. P. T. Hartendorp and J. N. H. Reek, *Acc. Chem. Res.*, 2018, **51**, 2115–2128.
28 L.-J. Chen, H.-B. Yang and M. Shionoya, *Chem. Soc. Rev.*, 2017, **46**, 2555–2576.
29 X. Jing, C. He, L. Zhao and C. Duan, *Acc. Chem. Res.*, 2019, **52**, 100–109.
30 S. Chakraborty and G. R. Newkome, *Chem. Soc. Rev.*, 2018, **47**, 3991–4016.
31 A. Goswami, S. Saha, P. K. Biswas and M. Schmittel, *Chem. Rev.*, 2020, **120**, 125–199.
32 S. Durot, J. Taesch and V. Heitz, *Chem. Rev.*, 2014, **114**, 8542–8578.
33 Z. He, W. Jiang and C. A. Schalley, *Chem. Soc. Rev.*, 2015, **44**, 779–789.
34 M. J. Hardie, *Chem. Soc. Rev.*, 2010, **39**, 516–527.
35 S. Pullen, J. Tessarolo and G. H. Clever, *Chem. Sci.*, 2021, **12**, 7269–7293.
36 Y. Li, H. Wang and X. Li, *Chem. Sci.*, 2020, **11**, 12249–12268.
37 Y. Domoto, M. Abe, K. Yamamoto, T. Kikuchi and M. Fujita, *Chem. Sci.*, 2020, **11**, 10457–10460.
38 Y. Domoto, M. Abe and M. Fujita, *J. Am. Chem. Soc.*, 2021, **143**, 8578–8582.
39 A. Kumar, R. Saha and P. S. Mukherjee, *Chem. Sci.*, 2021, **12**, 5319–5329.
40 P. Howlader, S. Mondal, S. Ahmed and P. S. Mukherjee, *J. Am. Chem. Soc.*, 2020, **142**, 20968–20972.
41 J.-H. Zhang, H.-P. Wang, L.-Y. Zhang, S.-C. Wei, Z.-W. Wei, M. Pan and C.-Y. Su, *Chem. Sci.*, 2020, **11**, 8885–8894.
42 K. Wu, K. Li, S. Chen, Y.-J. Hou, Y.-L. Lu, J.-S. Wang, M.-J. Wei, M. Pan and C.-Y. Su, *Angew. Chem., Int. Ed.*, 2020, **59**, 2639–2643.
43 X. Zhang, X. Dong, W. Lu, D. Luo, X.-W. Zhu, X. Li, X.-P. Zhou and D. Li, *J. Am. Chem. Soc.*, 2019, **141**, 11621–11627.
44 D. Luo, X.-Z. Wang, C. Yang, X.-P. Zhou and D. Li, *J. Am. Chem. Soc.*, 2018, **140**, 118–121.
45 M. D. Ludden, C. G. P. Taylor and M. D. Ward, *Chem. Sci.*, 2021, **12**, 12640–12650.
46 M. D. Ludden, C. G. P. Taylor, M. B. Tipping, J. S. Train, N. H. Williams, J. C. Dorrat, K. L. Tuck and M. D. Ward, *Chem. Sci.*, 2021, **12**, 14781–14791.
47 S. P. Argent, F. C. Jackson, H. M. Chan, S. Meyrick, C. G. P. Taylor, T. K. Ronson, J. P. Rourke and M. D. Ward, *Chem. Sci.*, 2020, **11**, 10167–10174.
48 J. Tessarolo, H. Lee, E. Sakuda, K. Umakoshi and G. H. Clever, *J. Am. Chem. Soc.*, 2021, **143**, 6339–6344.
49 H. Wang, K. Wang, Y. Xu, W. Wang, S. Chen, M. Hart, L. Wojtas, L.-P. Zhou, L. Gan, X. Yan, Y. Li, J. Lee, X.-S. Ke, X.-Q. Wang, C.-W. Zhang, S. Zhou, T. Zhai, H.-B. Yang, M. Wang, J. He, Q.-F. Sun, B. Xu, Y. Jiao, P. J. Stang, J. L. Sessler and X. Li, *J. Am. Chem. Soc.*, 2021, **143**, 5826–5835.
50 Y. Li, S. S. Rajasree, G. Y. Lee, J. Yu, J.-H. Tang, R. Ni, G. Li, K. N. Houk, P. Deria and P. J. Stang, *J. Am. Chem. Soc.*, 2021, **143**, 2908–2919.
51 C. T. McTernan, T. K. Ronson and J. R. Nitschke, *J. Am. Chem. Soc.*, 2021, **143**, 664–670.
52 S. Sudan, R.-J. Li, S. M. Jansze, A. Platzek, R. Rudolf, G. H. Clever, F. Fadaei-Tirani, R. Scopelliti and K. Severin, *J. Am. Chem. Soc.*, 2021, **143**, 1773–1778.
53 K. Omoto, S. Tashiro and M. Shionoya, *J. Am. Chem. Soc.*, 2021, **143**, 5406–5412.
54 J.-F. Ayme, J.-M. Lehn, C. Bailly and L. Karmazin, *J. Am. Chem. Soc.*, 2020, **142**, 5819–5824.
55 L. S. Lisboa, J. A. Findlay, L. J. Wright, C. G. Hartinger and J. D. Crowley, *Angew. Chem., Int. Ed.*, 2020, **59**, 11101–11107.
56 S. Samantray, S. Krishnaswamy and D. K. Chand, *Nat. Commun.*, 2020, **11**, 880.
57 D. Liu, M. Chen, K. Li, Z. Li, J. Huang, J. Wang, Z. Jiang, Z. Zhang, T. Xie, G. R. Newkome and P. Wang, *J. Am. Chem. Soc.*, 2020, **142**, 7987–7994.
58 S. Oldknow, D. R. Martir, V. E. Pritchard, M. A. Blitz, C. W. G. Fishwick, E. Zysman-Colman and M. J. Hardie, *Chem. Sci.*, 2018, **9**, 8150–8159.
59 M. Hardy, N. Struch, J. J. Holstein, G. Schnakenburg, N. Wagner, M. Engeser, J. Beck, G. H. Clever and A. Luetzen, *Angew. Chem., Int. Ed.*, 2020, **59**, 3195–3200.
60 A. N. Oldacre, A. E. Friedman and T. R. Cook, *J. Am. Chem. Soc.*, 2017, **139**, 1424–1427.

61 L. He, L.-X. Cai, M.-H. Li, G.-L. Zhang, L.-P. Zhou, T. Chen, M.-J. Lin and Q.-F. Sun, *Chem. Sci.*, 2020, **11**, 7940–7949.
62 L. Yang, X. Jing, B. An, C. He, Y. Yang and C. Duan, *Chem. Sci.*, 2018, **9**, 1050–1057.
63 S. Bai, L.-L. Ma, T. Yang, F. Wang, L.-F. Wang, F. E. Hahn, Y.-Y. Wang and Y.-F. Han, *Chem. Sci.*, 2021, **12**, 2165–2171.
64 Y. Lu, D. Liu, Y.-J. Lin and G.-X. Jin, *Chem. Sci.*, 2020, **11**, 11509–11513.
65 W. M. Hart-Cooper, C. Zhao, R. M. Triano, P. Yaghoubi, H. L. Ozores, K. N. Burford, F. D. Toste, R. G. Bergman and K. N. Raymond, *Chem. Sci.*, 2015, **6**, 1383–1393.
66 A. J. Plajer, F. J. Rizzuto, L. K. S. von Krbek, Y. Gisbert, V. Martinez-Agramunt and J. R. Nitschke, *Chem. Sci.*, 2020, **11**, 10399–10404.
67 S. M. Jansze, G. Cecot and K. Severin, *Chem. Sci.*, 2018, **9**, 4253–4257.
68 T. Tsutsui, L. Catti, K. Yoza and M. Yoshizawa, *Chem. Sci.*, 2020, **11**, 8145–8150.
69 X. Hu, S. Feng, J. Du, L. Shao, J. Lang, C. Zhang, S. P. Kelley, J. Lin, S. J. Dalgarno, D. A. Atwood and J. L. Atwood, *Chem. Sci.*, 2020, **11**, 12547–12552.
70 E. O. Bobylev, D. A. Poole III, B. de Bruin and J. N. H. Reek, *Chem. Sci.*, 2021, **12**, 7696–7705.
71 R. Sumida, Y. Tanaka, K. Niki, Y. Sei, S. Toyota and M. Yoshizawa, *Chem. Sci.*, 2021, **12**, 9946–9951.
72 V. Marti-Centelles, R. L. Spicer and P. J. Lusby, *Chem. Sci.*, 2020, **11**, 3236–3240.
73 C. Tan, J. Jiao, Z. Li, Y. Liu, X. Han and Y. Cui, *Angew. Chem., Int. Ed.*, 2018, **57**, 2085–2090.
74 J. Jiao, C. Tan, Z. Li, Y. Liu, X. Han and Y. Cui, *J. Am. Chem. Soc.*, 2018, **140**, 2251–2259.
75 J. Tian, L. Liu, K. Zhou, Z. Hong, Q. Chen, F. Jiang, D. Yuan, Q. Sun and M. Hong, *Chem. Sci.*, 2020, **11**, 9818–9826.
76 G. Mezei, C. M. Zaleski and V. L. Pecoraro, *Chem. Rev.*, 2007, **107**, 4933–5003.
77 B. M. Ahmed and G. Mezei, *Chem. Commun.*, 2017, **53**, 1029–1032.
78 M. Yoshizawa, M. Tamura and M. Fujita, *Science*, 2006, **312**, 251–254.
79 W. Cullen, M. C. Misuraca, C. A. Hunter, N. H. Williams and M. D. Ward, *Nat. Chem.*, 2016, **8**, 231–236.
80 Q.-Q. Wang, S. Gonell, S. H. A. M. Leenders, M. Duerr, I. Ivanovic-Burmazovic and J. N. H. Reek, *Nat. Chem.*, 2016, **8**, 225–230.
81 H. Takezawa, K. Shitozawa and M. Fujita, *Nat. Chem.*, 2020, **12**, 574–578.
82 D. M. Kaphan, M. D. Levin, R. G. Bergman, K. N. Raymond and F. D. Toste, *Science*, 2015, **350**, 1235–1238.
83 W. Cullen, A. J. Metherell, A. B. Wragg, C. G. P. Taylor, N. H. Williams and M. D. Ward, *J. Am. Chem. Soc.*, 2018, **140**, 2821–2828.
84 D. A. Poole III, S. Mathew and J. N. H. Reek, *J. Am. Chem. Soc.*, 2021, **143**, 16419–16427.
85 V. Martí-Centelles, A. L. Lawrence and P. J. Lusby, *J. Am. Chem. Soc.*, 2018, **140**, 2862–2868.
86 J. Wang, T. A. Young, F. Duarte and P. J. Lusby, *J. Am. Chem. Soc.*, 2020, **142**, 17743–17750.
87 K. Li, K. Wu, Y. L. Lu, J. Guo, P. Hu and C. Y. Su, *Angew. Chem., Int. Ed.*, 2022, **61**, e202114070.
88 H. Takezawa, T. Murase and M. Fujita, *J. Am. Chem. Soc.*, 2012, **134**, 17420–17423.
89 P. Mal, B. Breiner, K. Rissanen and J. R. Nitschke, *Science*, 2009, **324**, 1697–1699.
90 S. Hasegawa, S. L. Meichsner, J. J. Holstein, A. Baksi, M. Kasanmascheff and G. H. Clever, *J. Am. Chem. Soc.*, 2021, **143**, 9718–9723.
91 D. M. Kaphan, F. D. Toste, R. G. Bergman and K. N. Raymond, *J. Am. Chem. Soc.*, 2015, **137**, 9202–9205.
92 J. Wei, L. Zhao, C. He, S. Zheng, J. N. H. Reek and C. Duan, *J. Am. Chem. Soc.*, 2019, **141**, 12707–12716.
93 L. J. Jongkind, J. A. A. W. Elemans and J. N. H. Reek, *Angew. Chem., Int. Ed.*, 2019, **58**, 2696–2699.
94 J. Guo, Y.-Z. Fan, Y.-L. Lu, S.-P. Zheng and C.-Y. Su, *Angew. Chem., Int. Ed.*, 2020, **59**, 8661–8669.
95 X.-L. Tang, W.-H. Wang, W. Dou, J. Jiang, W.-S. Liu, W.-W. Qin, G.-L. Zhang, H.-R. Zhang, K.-B. Yu and L.-M. Zheng, *Angew. Chem., Int. Ed.*, 2009, **48**, 3499–3502.
96 B. Wang, B. Ma, Z. Wei, H. Yang, M. Wang, W. Yin, H. Gao and W. Liu, *Inorg. Chem.*, 2021, **60**, 2764–2770.
97 S. D. Bian, J. H. Jia and Q. M. Wang, *J. Am. Chem. Soc.*, 2009, **131**, 3422–3423.
98 D. Sun, G.-G. Luo, N. Zhang, R.-B. Huang and L.-S. Zheng, *Chem. Commun.*, 2011, **47**, 1461–1463.
99 C. Browne, W. J. Ramsay, T. K. Ronson, J. Medley-Hallam and J. R. Nitschke, *Angew. Chem., Int. Ed.*, 2015, **54**, 11122–11127.
100 W. A. Al Isawi, M. Zeller and G. Mezei, *Inorg. Chem.*, 2021, **60**, 13479–13492.
101 W. A. Al Isawi and G. Mezei, *Molecules*, 2021, **26**, 3083.
102 X. Li, J. Wu, C. He, R. Zhang and C. Duan, *Chem. Commun.*, 2016, **52**, 5104–5107.
103 A. Martinez-Camarena, A. Liberato, E. Delgado-Pinar, A. G. Algarra, J. Pitarch-Jarque, J. M. Llinares, M. Angeles Manez, A. Domenech-Carbo, M. G. Basallote and E. Garcia-Espana, *Inorg. Chem.*, 2018, **57**, 10961–10973.
104 A. Martinez-Camarena, P. A. Sanchez-Murcia, S. Blasco, L. Gonzalez and E. Garcia-Espana, *Chem. Commun.*, 2020, **56**, 7511–7514.
105 J.-W. Wang, W.-J. Liu, D.-C. Zhong and T.-B. Lu, *Coord. Chem. Rev.*, 2019, **378**, 237–261.
106 J.-W. Wang, C. Hou, H.-H. Huang, W.-J. Liu, Z.-F. Ke and T.-B. Lu, *Catal. Sci. Technol.*, 2017, **7**, 5585–5593.
107 F. Ibukuro, T. Kusukawa and M. Fujita, *J. Am. Chem. Soc.*, 1998, **120**, 8561–8562.
108 G. Liu, Y. Di Yuan, J. Wang, Y. Cheng, S. B. Peh, Y. Wang, Y. Qian, J. Dong, D. Yuan and D. Zhao, *J. Am. Chem. Soc.*, 2018, **140**, 6231–6234.
109 C. Ngai, H.-T. Wu, B. da Camara, C. G. Williams, L. J. Mueller, R. R. Julian and R. J. Hooley, *Angew. Chem., Int. Ed.*, 2022, **61**, e202117011.